

Comparative study of different scalable routes to synthesize graphene oxide and reduced graphene oxide

A. Romero^a

M.P. Lavin-Lopez^{b, *}

pradolavin@graphenano.com

L. Sanchez-Silva^a

J.L. Valverde^a

A. Paton-Carrero^a

^aUniversity of Castilla-La Mancha, Department of Chemical Engineering, Avenida Camilo Jose Cela 12, 13071, Ciudad Real, Spain

^bGraphenano S.L., Calle Pablo Casals 13, 30510, Yecla, Murcia, Spain

*Corresponding author.

Abstract

Graphene oxide is considered one of the most significant material due to its capability of be a reliable and potentially scalable precursor of graphene. Several processes of graphene mass production are getting involved into very polluting oxidants, toxic gases emissions, explosions and deflagrations or even long-time reactions. In the present work, two different routes were carried out in order to obtain reduced graphene oxide. On the one hand, a modification of *Improved Hummers method* whose modifications efficiently reduce the reaction time and the amount of chemical reagents. On the other hand, an environmentally friendly, fast and economic method which use potassium ferrate as oxidizing agent. Products obtained by both methods were characterized with different techniques: Raman spectroscopy, Scanning Electron Microscopy, FT-IR, elemental analysis (EDX), X-Ray Diffraction, Thermogravimetric Analysis, DSC and particle size analyzer. Results acquired by the modified Improved Hummers Method are more effective than that one based on potassium ferrate as oxidizing agent. However, in spite of the lower oxidation degree achieved in the last one, the resulting material suffered important physicochemical structural changes which are explained in detail. These changes could be of interest for anticipating future applications of graphene-based materials.

Keywords: Graphene oxide; Oxidation; Improve *Hummers* method; Potassium ferrate; Functional oxygen groups

1 Introduction

Graphene is considered the world's strongest and thinnest material, in addition to be a very good heat and electricity conductor. Traditional methods to produce graphene include mechanical exfoliation, Chemical Vapor Deposition or thermal expansion but none of them are attractive from the commercial point of view due to its low yield or the poor quality of the retrieved product [1]. Graphite and graphene oxide are the most important graphene allotropes. Graphite oxide is obtained by generation of oxygenated functional groups on the surface and edges of graphite which, after its layer expansion, provides graphene oxide. Nowadays, graphene oxide reduction (via chemical or thermal routes) seems to be the best method to synthesize graphene at industrial scale [2] although, as a consequence of the experimental procedure followed, some defects remain in the final structure of the product.

Graphite oxide can be synthesized by either Brodie, Staudenmaier, or Hummers method and its variations, namely Modified Hummers Method or Improved Hummers Method [3]. Among them, Improved Hummers Method is characterized by its both lower toxicity and several advantages in terms of the resulting products. Even so, the oxidation protocol associated to the *Improved Hummed Method* clearly depends on the abundant use of strong acids (leading to subsequent environmental issues), high treatment times and tedious purification processes, which results in high manufacture costs [4]. These reasons among others make the industrial commercialization of graphite oxide and its derivative products to be limited.

In previously papers, optimization of the Improved Hummers Method (as reported in Literature [3]) which use graphite as the raw material and KMnO_4 and H_2SO_4 as chemical reagents to produce the oxidation of graphite was reported. Chen et al. [5] proposed in 2013 the elimination of NaNO_3 for the reaction and H_3PO_4 for graphite oxide washing and demonstrated the disposal of waste water. Lavin-Lopez et al. [6] showed that the oxidation time could be

reduced (from 12 to 3 h), removing the coagulation step and the use of H_3PO_4 during the oxidation step should. The graphite oxide production per batch is increased as well (by increasing the amount of graphite that could be treated from 3 to 15 g, while keeping the graphite/ KMnO_4 ratio constant), without significantly altering the final product (graphite oxide) characteristics. In other words, a significant reduction in the synthesis costs could be achieved at industrial level.

On the other hand, some studies that allow a green synthesis of GO have been recently published. Yu et al. [4] reported a green method for the production of GO using a ferro-induced procedure in absence of acid media. Peng et al. [7] also managed to synthesize GO using a green Ferrate-based procedure but they could not avoid the use of H_2SO_4 . In both cases, the protocols of synthesis followed are simple, low cost, time saving and environmentally acceptable, which should facilitate the process scale up.

Although it is clear that the use of different oxidation routes has an impact on the final product properties (exfoliation level, number of layers, sheets size, number of defects, sp^2 and sp^3 domains, etc. [8]), there are a lack of studies that compares all or part of them. In this context, the present study raises graphite oxidation procedures using novel conditions and/or oxidants to allow the chemical exfoliation of graphite and after reduction to obtain *Reduced Graphene Oxide*. In this sense, two different routes were followed to obtain *graphene oxide*. Firstly, high quality graphite and graphene oxide were synthesized by using the *Improved Hummers method* in which, some modifications were carried out in order to reduce the reaction time and the quantities of chemical reagents required during the synthesis procedure [4]. Secondly, graphite and graphene oxide were produced via an environmentally friendly, fast and economic method based on the use of Potassium Ferrate as the oxidizing agent, this method will be called *Ferrate Method*.

The study of this ferrate-based method and the comparison carried out in the present work, at the expense of others more harmful and dangerous such as, Tour, Brodie [9], Hummers [10] and other methods which used potassium chromate [11] or Fenton oxidation [4], could provide a new line of investigation being possible the ecofriendly and massive production of graphene oxide.

2 Materials and methods

2.1 Materials

Graphite powder with a particle size $<20\ \mu\text{m}$, KMnO_4 (purity of 99%), H_2SO_4 (purity of 96%) and HCl (purity $\geq 37\%$) were supplied by Sigma-Aldrich. H_2O_2 (purity of 33%). Ethanol (purity of 99.5%) were supplied by Panreac. K_2FeO_4 (purity of 92%) was supplied by Lab Seeker.

2.2 Synthesis of Graphite Oxide (GrO), Graphene Oxide (GO) and Reduced Graphene Oxide (RGO)

Graphite oxide was firstly synthesized following the *Improved Hummers Method* with some modifications [12]. A mixture of 15 g of graphite and 45 g of potassium ferrate (ratio 1:3) was slowly added into a vessel with 400 mL of H_2SO_4 . The reaction is very violent so it was necessary to maintain the temperature at $50\ ^\circ\text{C}$ under vigorous stirring in order to avoid deflagrations. After 3 h of stirring, it was added 400 g of flake ice and 3 mL of oxygenated water (20% in relation to graphite amount) in order to stop the graphite oxidation and reduce the dissolution temperature. Next, the mixture was filtered under vacuum and washed with 200 mL of distilled water for the elimination of non-oxidized graphite, 200 mL of hydrochloric acid to remove the metallic ions and 200 mL of ethanol in order to reduce the later drying process. To conclude, the cake was dried overnight at $100\ ^\circ\text{C}$ in a drying oven. Graphite oxide synthesized using the modified *Improved Hummers Method* was named to as GrO-H.

Also, graphite oxide was synthesized using the *Ferrate Method*. In this method 10 g of graphite and 60 g of potassium ferrate (ratio 1:6) was mixed. This mixture was added to 400 mL of sulfuric acid in a vessel. The reaction was held under vigorous stirring at room temperature and atmospheric pressure. The reaction was kept at this condition for 1 h. After this time, the reaction was filtered with a vacuum pump. Then, it was washed with distilled water until the reaction pH reach neutral pH ($\sim 3\ \text{L}$). The cake obtained was dried during 3 h at 70° in a drying oven. The powder was dried during 3 h at 70° . Graphite oxide synthesized using *Ferrate Method* was named to as GrO-F.

Graphene oxide synthesis was carried out by graphite oxide exfoliation. Thus, 1 g/L of graphite oxide dissolution was prepared by mixing 800 mg of graphite oxide and 800 mL of deionized water. Then, the mixture was introduced in a cooling jacketed reactor to maintain the solution at room temperature. The mixture was sonicated for 2 h under stipulated conditions (1 cycle and 50% amplitude) in order to separate the graphene sheets of graphite oxide and obtain graphene oxide. The final mixture was centrifuged at 12000 rpm for 1 h to precipitate the graphene oxide. Finally, the obtained solid was dried at $80\ ^\circ\text{C}$. Samples were named GO-H and GO-F.

The chemical reduction was performed by using hydrazine monohydrated as reduction agent (ratio 1.1). To do it, it was taken 800 mL of graphene oxide solution (1 g/L) before the centrifugation and it was added 800 mL of hydrazine monohydrated. The mixture was maintained under constant agitation at $90\ ^\circ\text{C}$ in a closed stirring reactor for 3 h. When the time is up the solution was centrifuged at 10000 rpm during 30 min in order to precipitate the product (RGO-H/RGO-F). Then, the precipitated was washed with deionized water until neutral pH to eliminate the remaining hydrazine ($\sim 3\ \text{L}$). The product obtained was dried at $80\ ^\circ\text{C}$ during 4 h in a drying oven [13].

2.3 Characterization techniques

Fourier transform infrared (FTIR) spectra analyses were carried out on a SPECTRUM TWO spectrometer (Perkin Elmer, Inc), the analysis range was between 400 and 5000 cm^{-1} with 4 cm^{-1} of resolution. Raman spectrums were obtained with a SENTERRA spectrometer using an excitation wavelength of 532 nm. Thermogravimetric analyses (TGA) data were recorded on a METTLER TOLEDO TGA/DSC1 instrument, the samples were heating from room temperature to 1000 $^{\circ}\text{C}$ (10 $^{\circ}\text{C min}^{-1}$) in air atmosphere. The morphology of the samples was observed with Scanning Electron Microscopy (SEM) (Phenom ProX) and elemental analyses were carried out using the EDX software of the SEM equipment. The calorimetric analyses were performed in a METTLER TOLEDO DSC2 instrument at a heating rate of 5 $^{\circ}\text{C min}^{-1}$ under nitrogen atmosphere. The particle size was measured by using a Mastersizer 2000 to whom attached a module -Hydro-for dissolution measures. X-Ray diffraction analyses were performed on a diffractometer (PHILIPS, PW-1711) with $\text{CuK}\alpha$ radiation ($\lambda = 1.5404 \text{ \AA}$). Attending to X-Ray diffractogram several crystallographic parameters were calculated, such as interlaminar space (d_{002}); crystal stack height (L_c); in-plane crystallite size or layer size (L_a) and, number of graphene layers in the crystal (N_c) [14-17]:

$$d_{002} = \frac{\lambda}{2 \cdot \sin\theta_1}; L_c = \frac{k_1 \cdot \lambda}{FWHM \cdot \cos\theta_1}; L_a (nm) = \frac{k_2 \cdot \lambda}{FWHM \cdot \cos\theta_2}; N_c = \frac{L_c}{d_{002}}$$

where:

- λ , radiation wavelength ($\lambda = 0,15404 \text{ nm}$)
- θ_1 , [002] and [001] diffraction peak position ($^{\circ}$)
- θ_2 , [100] diffraction peak position ($^{\circ}$)
- k_1 , Form factor ($k = 0,9$)
- k_2 , Warren Form Factor constant ($k = 1,84$)
- $FWHM$, Width at half height of the corresponding diffraction peak (rad)

3 Results and discussion

Table 1 shows the elemental analysis, i.e., the oxygen and carbon atoms content (wt.%) corresponding to the different graphene-based materials. Graphite, the non-oxidized raw material, is composed by 100% of carbon atoms. After the oxidation process, yielding graphite oxide, sample GrO-H showed a 45% of the oxygen atoms that were present as oxygen functional groups whereas just 16% of them were present in sample GrO-F. Graphene oxide (GO), obtained after GrO exfoliation by sonication, always showed a similar oxygen content as that of sample GrO regardless of the oxidation procedure, which seems logical due to sonication is a physical process that should not imply any change in the chemical composition. After the chemical reduction process with hydrazine, oxygen functional groups were reduced from 45% to 28% in the case of RGO-H and, from 16% to 11% in the case of sample RGO-F.

Table 1 Atomic composition (%) of graphite, GrOs, GOs and RGOs materials.

alt-text: Table 1

Sample	C (%)	O (%)	Ratio C/O
Graphite	100	0	–
GrO-H	55	45	1.14
GO-H	56	44	1.06
RGO-H	72	28	2.55
GrO-F	84	16	5.47
GO-F	85	15	5.72
RGO-F	89	11	8.35

It can be verified from the results that the procedure based on the graphite oxidation following the modified *Improved Hummers Method* is much more efficient in terms of incorporation of oxygen groups in structure. Thus, the influence of incorporating different functional groups in the structure on properties such as crystallinity, thermal resistance, exfoliation degree, number of graphene layers, etc., was studied in detail.

Fig. 1 shows the TGA and DTG curves corresponding to graphite (G) and graphite oxide (GrO) and graphene oxide (GO) prepared by following both the modified *Improved Hummers Method* and the *Ferrate Method*. TGA curve of graphite confirmed the high thermal stability of this material, which did not start its decomposition until around 700 °C, losing around 94% of its mass at 850 °C [18]. On the other hand, samples GrO-H and GO-H showed similar TGA curves where three different weight loss steps can be differentiated. The first one (I), appearing between 0 and 275 °C, was mainly due to the elimination of both water solvent molecules and the thermally induced decomposition of the more labile oxygen functional groups and subsequent release of steam and gases (CO, CO₂). This gas formation process requires overcoming the strong interlayer bonding [19]. According to Eigler et al. [20], GO exhibits also sulfonic groups which could be located above and below the carbon skeleton or at the edges of the GO flakes and, decompose at temperatures of around 250 °C. The second weight loss step (II), occurring approximately between 275 and 475 °C, is associated to the removal of the more stable oxygen groups, leading to similar results for samples GrO-H and GO-H. Finally, a third step (III), occurring at temperatures ranging from 475 to 500 °C, was a consequence of the material thermal degradation, losing around 33% of the remaining mass. Removal of oxygenated functional groups is linked to the CO and CO₂ evolution involving the generation of atomic vacancies and voids into the carbonaceous structure. Although the elimination of an isolated functional group on graphene is energy costly, the process is enhanced, both thermodynamic and kinetically, in presence of more oxygen functional groups closely located. In other words, the group energy stabilizes both the final structure and transition states [21]. High oxygen density, as observed in samples GrO-H and GO-H, favors the low temperature elimination (step I) of an important part of the oxygen functional groups present in the structure. However, after oxygen removal at low temperatures, the remaining oxygen functional groups are most likely to be in the form of (more or less) isolated groups, thus requiring much higher temperatures for its removal [22].

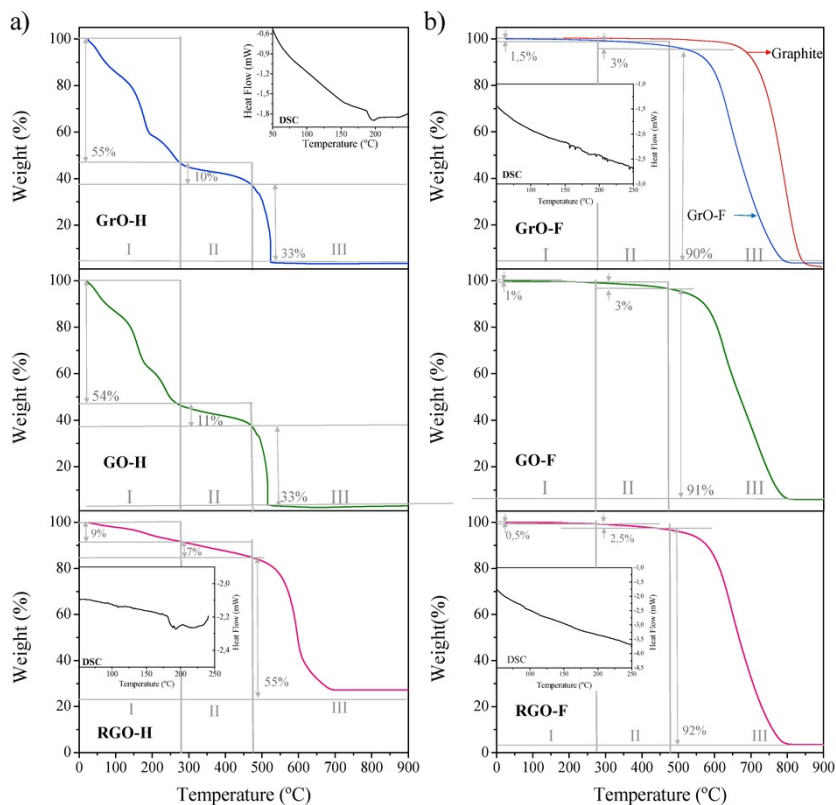


Fig. 1 TGA analysis corresponding to a) samples prepared by the modified *Improved Hummers Method* and b) samples prepared by the *Ferrate Method*. (Operational conditions: air atmosphere, temperature range: 0-1000 °C, 5 °C/min).

alt-text: Fig. 1

TGA profile of graphite and graphene oxide synthesized using the *Ferrate Method* showed similar thermal behavior as that of the raw graphite but in this case the degradation was shifted to lower temperatures. Thus, samples GrO-F and GO-F started to oxidize at around 475 °C and was completely burn off at 780 °C; being 700 and 850 °C for raw graphite, respectively. This high thermal reactivity is a consequence of the distorted carbon structure induced by the small presence of oxygen groups introduced during the synthesis process. Sample GrO-F has a layered morphology with some oxygen-containing functionalities that weakens the Van der Waals forces between layers. Thus, the

hexagonal carbon basal planes in the multilayered stacks structure of graphene oxide will be disrupted, thus accelerating the process of weight losing [23]. On the other hand, samples GrO-F and GO-F were thermally stable in the range of temperatures from room temperature to 275 °C (first step). A small weight loss at the second step (3%) ranging from 275 to 475 °C was found in samples GrO-F and GO-F due to the detachment of functional organic groups from the graphite scaffold. The lower thermal stability showed in samples GrO-F and GO-F compared to that of graphite could be also associated to the presence of fewer layers generated after **after** the exfoliation of the parent material [24].

DSC scans are inset in Fig. 1. As observed, an exothermic peak at around 190 °C appeared for sample GrO-H, which is associated to the thermal decomposition and exfoliation of graphene oxide (melting point of the γ phase crystals [25]). Around 37% weight losses are associated to the exothermic DSC peak, roughly quantifying the amount of decomposed molecules. This exothermic peak could not be clearly appreciated in sample GO-F.

TGA results for chemically reduced samples confirmed the high reduction power of hydrazine. Thus, sample RGO-H showed a minimum weight loss in step (I) ($\approx 9\%$), confirming the elimination of the most labile oxygen groups after the reduction process. On the other hand, weight loss corresponding to step (II) was of around 7%, being the weight loss associated to step (III) 55%. On the other hand, sample RGO-F showed a TGA profile quite similar to that of sample GrO-F, although, thermal degradation may occur at slightly lower temperatures. Finally, it is important to note that both GrO-H/GO-H and GrO-F/GO-F exhibited identical residual weight of around 4% and 6%, respectively. Nevertheless, after reduction, sample RGO-H exhibited a residual char weight of 25% while in sample RGO-F this value was close to 6%, indicating that the *Ferrate Method* could be considered an impurity-free method to obtain graphene based materials.

Thermogravimetric analysis results were corroborated by FTIR (Fig. 2). Regarding GrO-H sample prepared by the *Optimized Improved Hummers Method* oxidation, several functional groups were incorporated into the material structure [26]. The most intense peak, attributed to the O-H stretching vibrations of hydroxyl group sand water molecules, occurs in the range 3000-3600 cm^{-1} , also being observed the deformation vibration modes of O-H groups around 1430 cm^{-1} . A band located at 2890 cm^{-1} corresponds to alkene groups (C - H); a band appearing at around 1710-1760 cm^{-1} was associated to the C=O stretching vibration of a carbonyl group; a band located at approximately 1630 cm^{-1} was attributed to the C=C skeletal vibration of the graphene planes (unoxidized graphitic domains) [27]; a peak appearing at 1220-1230 cm^{-1} was in turn attributed to the stretching vibration of epoxy C-O-C group, and, a band at around 1050-1100 cm^{-1} was finally attributed to the alkoxy C-O stretching vibration (carboxyl group) [25,28,29]. Consequently, FTIR identified similar functional groups present in the GrO-H and GO-H structures (the latter not shown), confirming that the chemical identity of the bulk materials. After the reduction process, it was confirmed that the broad band corresponding to hydroxyl groups (centered around 3400 cm^{-1}) disappeared due to that hydrazine attacks OH groups by nucleophilic substitution [30], causing different hydrogen bond rearrangements [31]. Furthermore, a new small band appearing around 3000 cm^{-1} could be appreciated due to the tendency of oxygen functional groups to form complex structures with nitrogen. Thus, *Chua et al.* [32] demonstrated that carbonyl groups, which were readily removed, formed the corresponding hydrazine complexes under hydrazine reaction. They also demonstrated in a computational study that the hydrazine reduction removes favorably OH groups present in graphene oxide basal plane but not carboxylic groups, which agrees with the results obtained in the present work. Other oxygen functional groups, such as epoxy groups, were also partially removed after hydrazine reduction with the subsequent weakened of the corresponding absorption bands (Fig. 2).

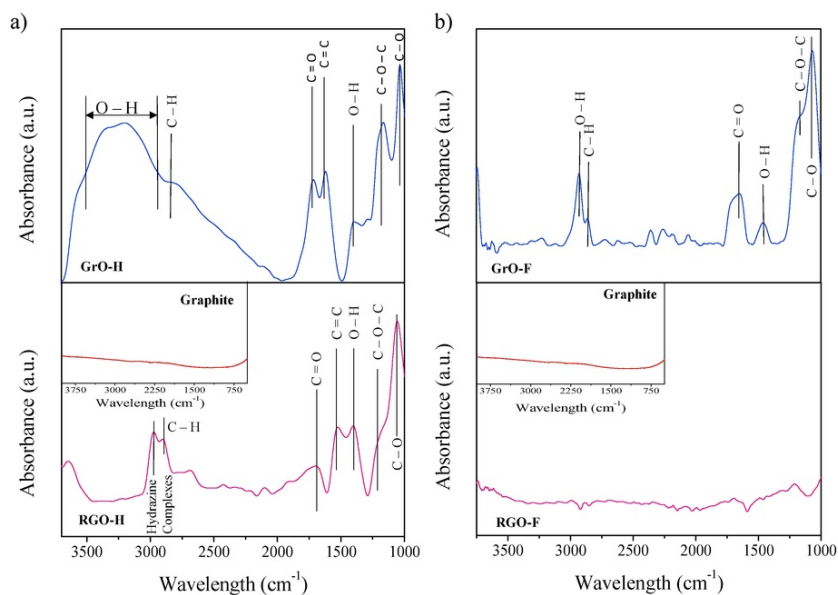


Fig. 2 FTIR spectra of graphite oxide and reduced graphene oxide samples synthesized by a) the modified *Improved Hummers Method* and b) the *Ferrate Method*. (Operational conditions: room temperature, wavelength range: 1000-3750 cm^{-1}).

alt-text: Fig. 2

Comparing and summarizing the results obtained by FTIR and TGA, it could be affirmed that the more labile oxygen groups are hydroxyl and carbonyl ones whereas the more stable oxygen groups are mainly carboxyl and epoxy ones. Note that the conjugated π -orbital system of the original graphite could have been destroyed during oxidation and, as a consequence, carboxyl and epoxy functional groups may be inserted into the carbon skeleton of samples GrO-H and GO-H [33]. On other hand, the presence of the C=C band showed the remaining sp^2 character [34].

Regarding the *Ferrate Method* oxidation, FTIR spectra also showed several functional groups in the structure of the material. The most intense bands corresponded to alkoxy (C - O) and epoxy groups (C - O - C). Also, hydroxyl (O-H) and carbonyl (C=O) groups occurred. As mentioned before, FTIR spectra of GrO-F and GO-F (not shown) were similar due to the method used to exfoliate the graphite oxide into graphene oxide is physical (not chemical) in nature. After the reduction, it was not possible to observe any oxygen functional group; consequently, a FTIR spectra similar as that of graphite was obtained.

Finally, it is important to note that the intensity of the wide peak associated to the C-OH stretching vibration (forming hydrogen bonds between GO layers and between GO and water molecules and causing in turn the hydrophilic moieties of the sample) is closely related to the oxygen content in the samples [25].

Materials were analyzed by Raman spectroscopy in order to characterize their structure in terms of establishing the number of graphene layers and fixing lattice defects (Fig. 3 and Table 2).

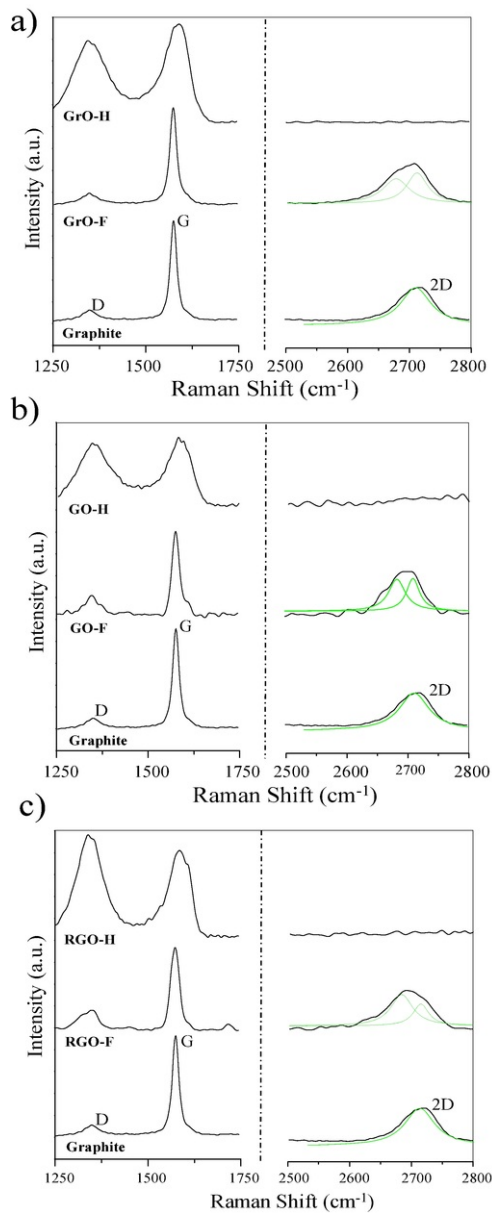


Fig. 3 Raman spectra of a) graphite oxide, b) graphene oxide and, c) reduced graphene oxide. (Operational conditions: room temperature, spectra range: 1000-3000 cm⁻¹, wavelength: 532 nm).

alt-text: Fig. 3

Table 2 Raman spectra peak positions, I_D/I_G and I_{2D}/I_G and L_D values of graphite, GrOs, GOs and RGOs materials.

alt-text: Table 2

Sample	D peak (cm ⁻¹)	G peak (cm ⁻¹)	FWHM G peak (cm ⁻¹)	2D peak (cm ⁻¹)	FWHM 2D peak (cm ⁻¹)	I_D/I_G	I_{2D}/I_G	L_D (nm)
--------	----------------------------	----------------------------	---------------------------------	-----------------------------	----------------------------------	-----------	--------------	------------

Graphite	1344	1572	20	2708	65	0.,11	0.43	29.52
GrO-F	1345	1576	24	2701	80	0.13	0.45	27.79
GO-F	1348	1576	25	2700	81	0.23	0.45	21.53
RGO-F	1348	1576	28	2692	85	0.24	0.45	20.61
GrO-H	1346	1592	80	-	-	0.84	-	10.99
GO-H	1346	1584	81	-	-	0.91	-	10.56
RGO-H	1342	1589	89	-	-	1.17	-	9.33

All samples prepared using the *Ferrate Method* (GrO-F/GO-F/RGO-F) exhibited the three typical bands related to graphite-based structures: the first one is the in-plane vibration of sp^2 carbon atoms (G band) at around 1576 cm^{-1} and the second one is the band associated to the presence of defects in the graphitic structure (D band) at around 1345 cm^{-1} [35]. And, the third one, the 2D band originated from the second order double resonant Raman scattering from the zone boundary at around 2700 cm^{-1} . Nevertheless, it is possible to observe that those samples obtained using the modified *Improved Hummers Method* (GrO-H/GO-H/RGO-H) showed only G and D bands. 2D peak was not visible in these samples as consequence of the more extensible oxidation taking place during the GrO-H synthesis.

As observed, GrO-F showed a I_{2D}/I_G ratio quite similar to that of graphite. On the other hand, according to previous studies [36], the number of layers of the resulting material could be identified from the position of the 2D Raman band. Thus, the smaller the 2D peak position, the lower the number of layers [37]. In addition, the 2D peak becomes wider [38]. Obtained results corroborate that after performing the oxidation of graphite with the *Ferrate Method* the number of graphene layers lightly decreased in sample GrO-F (see Table 2 and 2D peak position and FWHM). The lightly higher I_D/I_G ratio associated to sample GrO-F, if compared to that of graphite, would indicate the presence of a higher amount of defects and a lightly lower degree of graphitization. In addition, the increase of the G band FWHM in sample GrO-F, if compared again to that of graphite, revealed the presence of sp^3 carbon. Structural defects are introduced by the attachment of functional groups, such as hydroxyl or epoxy, on the carbon skeleton [29]. After sonication to produce graphene oxide (GO-F), Raman results were quite similar except that the 2D band shifted to lower values indicating that in this case the number of graphene layers decreased because of the graphite oxide exfoliation whereas the I_D/I_G ratio considerably increased due to the increase of the defects density. Note that the 2D peak deconvolution clearly indicates that these peaks move to lower Raman positions in this order: GrO-F > GO-F > RGO-F. Finally, after the reduction of sample RGO-F, the I_D/I_G ratio increases, clearly indicating that during the chemical reduction process the formation of vacancies and defects in the carbon lattice, such as five and seven membered carbon rings, took place [11].

On the other hand, the small shift to higher energies of the G band in sample GrO-H, if compared to that in sample GrO-F, would indicate that sample GrO-H would have fewer number of layers than sample GrO-F. On the other hand, the D band was much wider and the I_D/I_G ratio much higher in sample GrO-H spectrum than in that of sample GrO-F as a consequence of the structural imperfections induced by the attachment of higher amount of hydroxyl and/or epoxy groups on the carbon surface [39]. After the reduction process, the high I_D/I_G ratio was maintained and even lightly increased, showing the persistency of structural defects despite some oxygen functional groups were removed. These findings demonstrate that the introduction of more oxygen functional groups during the oxidation process results in the formation of more defects and vacancies in the final product, being impossible to entirely rearrange the carbon lattice as will be also commented below (XRD discussion) [29]. Finally, the distance between defects was estimated (as $LD = \sqrt{C(\lambda)/(ID/IG)}$, being $C(\lambda) = 102\text{ nm}^2$ [40]), demonstrating that a deeper oxidation occurs in samples prepared by the modified *Improved Hummers Method*.

XRD is one of the most popular technique to identify structural arrangements, oxidation degree and purity of graphite and graphene-based materials [41]. The XRD patterns and characteristic parameters of graphite and the corresponding oxidized and reduced samples are shown and listed in Fig. 4 and Table 3, respectively. Regarding graphite, a single sharp peak at 26.5° was observed which was ascribed to a [002] graphite face corresponding to an interlayer distance of 0.34 nm. Regarding sample GrO-H, a typical diffraction peak associated to graphite oxide ([001] peak) was observed at around 10° ; peak at 26.6° disappeared as a consequence of the complete oxidation of graphite [42]. Thus, the incorporation of different intercalated oxygen functional groups such as hydroxyl, epoxy, carbonyl and carboxyl groups which break the extended π -bond conjugated system of graphite, improving the GO hydration and exfoliation, is responsible for the 2.6 times larger interlayer spacing observed for sample GrO-H [43,44].

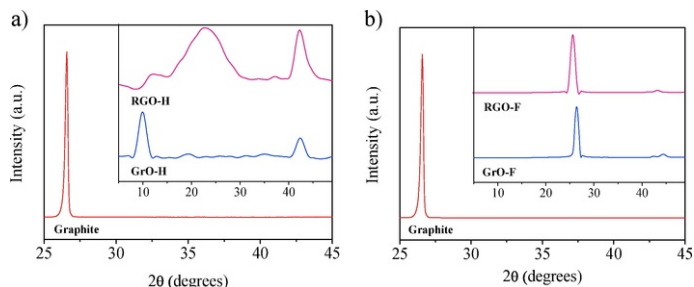


Fig. 4 XRD of graphite, GrO and, RGO corresponding to a) samples prepared by the modified *Improved Hummers Method* and, b) samples prepared by the *Ferrate Method*. (Operational conditions: room temperature, degrees range: 0 - 40°, λ : 1,5404 Å).

alt-text: Fig. 4

Table 3 Characteristic of graphite, GrO and RGO via XRD method.

alt-text: Table 3

Sample	FWHM (°)	d_{002} (nm)	L_c (nm)	L_A (nm)	Number Layers
Graphite	0.22	0.34	37.10	37.10	111
GrO-H	1.42	0.89	5.62	9.73	6
GrO-F	1.00	0.35	16.32	12.99	48
RGO-H	7.66	0.37	1.06	7.80	3
RGO-F	1.20	0.34	6.80	9.74	20

FWHM: Full width at half-maximum corresponding to [002] peak for graphite/GrO-F or [001] peak for GrO-H.

d_{002} : interlayer distance.

L_c , L_A : mean crystallite diameters.

Number layers: average number of sheets in crystallite (L_c/d_{002}).

On the other hand, after the oxidation procedure using *Ferrate Method*, graphite diffraction peak at 26.6° appeared displaced at slightly lower (but very close) 2θ values than that of graphite. Consequently, both materials showed similar d-spacing values. In other words, XRD analysis showed that the graphitic structure remained in sample GrO-F as consequence of the low oxidation degree [45]. Nevertheless, XRD signals in sample GrO-F were broader and decreased in intensity, which has been related to the fact that the crystallites sizes diminishing upon oxidation [1] as it can be corroborated by FWHM values listed in Table 3. It was calculated that the crystallites height (L_c) decreased after oxidation from 37 nm in graphite to 5.6 and 16.3 nm in samples GrO-H and GrO-F, respectively. On the other hand, the layer size of the crystallites (L_A) were determined to be 10 and 13 nm for samples GrO-H and GrO-F, respectively. Thus, the reduction in the crystallite sizes depends on the oxidation degree.

After the reduction process, the hydrophilic character of GrO-H/GO-H was minimized due to the removal of some oxygen functional groups and entrapped water molecules from the basal plane. This way, the initial graphitic structure was almost restored in sample RGO-H. XRD pattern associated to sample RGO-F was quite similar to that of sample GrO-F. Thus, it was not possible to appreciate the restoration of the initial graphitic structure since it was practically unaffected. Nevertheless, in both cases a broader reflection (compared to that of samples without reduction or the raw graphite) centered at around $2\theta = 24^\circ$ in the diffraction patterns, would indicate the formation of graphene nanosheets with fewer number of layers. As observed, crystal domains (L_c and L_A) decreased in both cases after chemical reduction due to the increasing structural disorder, which agreed well with RAMAN results.

Morphologies of aggregates derived from the parent graphite and its oxidized counterparts are shown in the SEM images of Fig. 5. Graphite morphology appears to be like compact stacks with well-defined edges because of the Van der Waals forces which hold its layers together. On the other hand, oxidized graphene based materials showed more wrinkled agglomerates with a more visible layer arrangement as consequence of the layer expansion. After oxidation by the modified *Improved Hummers Method*, the laminated structure of graphite was destroyed, making evident the GO structure delamination. However, after oxidation using the *Ferrate Method*, sheets were not extensively

exfoliated due to the incomplete oxidation achieved with this method. Upon reduction, samples exhibited similar aggregated morphology, being visible the layered arrangement in the SEM images [29].

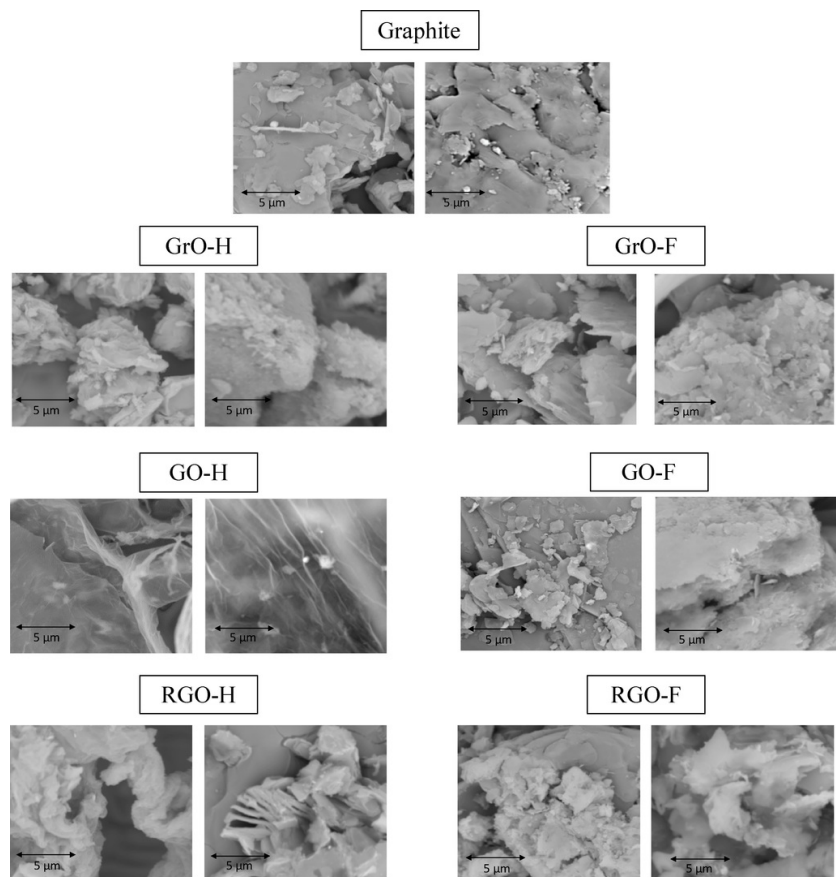


Fig. 5 SEM images of powder graphite and graphene based materials. a) Graphite; b) GrO-H; c) GrO-F; d) GO-H; e) GO-F; f) RGO-H; g) RGO-F. (Operational conditions: vacuum atmosphere, 15 kV, 2000X).

alt-text: Fig. 5

Another way of quantifying the exfoliation degree of the different samples consist of determining the particle size of the dried samples dispersed in water. Thus, quantitative evaluation of dispersion particle size (using a particle size analyzer) is shown in Table 4. As observed, the measured particle size gradually increased. Consequently, the particle size distribution became wider (not shown), mainly after graphite oxide sonication, which has been ascribed to the exfoliation of graphite oxide into graphene oxide nanosheets [46,47]. In other words, the dispersion of dry powder graphene in water leads to the occurrence of aggregates or precipitates, which was associated to strong inter-sheet van der Waals attractions, [42]. The lower increase in the particle size after sonication of graphite oxide using the Ferrate Method would again confirm the lower exfoliation level observed.

Table 4 Particle size distribution of GrO and GO samples.

alt-text: Table 4

Sample	D ₁₀ (μm)	D ₅₀ (μm)	D ₉₀ (μm)
Graphite	8.8	21.6	44.8
GrO-H	10.4	30.8	62.6
GrO-F	22.1	45.0	100.0
GO-H	22.1	45.0	100.0
GO-F	22.1	45.0	100.0
RGO-H	22.1	45.0	100.0
RGO-F	22.1	45.0	100.0

GO-H	33.1	153.2	473.9
GrO-F	10.5	25.9	48.8
GO-F	13.4	34.8	73.4

D₁₀, D₅₀ and, D₉₀ are particles sizes at which the percentages 10%, 50% and, 90% of the sample are below this given size.

4 Conclusions

Currently, Graphene Oxide (GO) is one of the most important carbon nanomaterial, being a potentially scalable precursor of graphene. Results have showed that graphene oxide obtained by the optimized *Improved Hummers Method*, which used potassium permanganate as oxidizing agent, was much more effective as far as the degree of oxidation is concerned, than that one obtained by using potassium ferrate as oxidizing agent. However, graphene oxide obtained by the second approached, presented remarkable physico-chemical changes compared to that of graphite (raw material) and GO obtained by the optimized *Improved Hummers Method*. Comparing both oxidation procedures, it can be concluded that, under a rigorous optimization of the synthesis conditions, potassium ferrate procedure could be a safe, time-saving, low cost, environmentally friendly and industrially viable alternative to traditional synthesis methods of graphene oxide. From the application point of view, all those properties derived of a less oxidized and less defective material, could open a new field in the future application of graphene-based materials.

Acknowledgements

The present work was performed within the frame of the NANOLEAP project. This project has received funding from the [European Union's Horizon 2020 research and innovation program](#) under grant agreement No [646397](#).

References

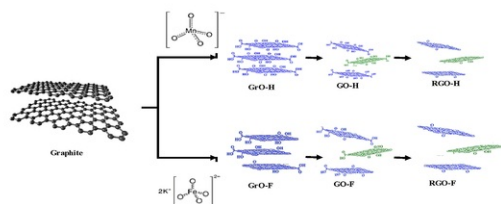
- [1] U. Saha, R. Jaiswal and T.H. Goswami, A facile bulk production of processable partially reduced graphene oxide as superior supercapacitor electrode material, *Electrochim. Acta* **196**, 2016, 386–404.
- [2] M. Ciszewski and A. Mianowski, Survey of graphite oxidation methods using oxidizing mixtures in inorganic acids, *Chemik* **1**, 2013, 267–274.
- [3] D.C. Marcano, D.V. Kosynkin, J.M. Berlin, A. Sinitskii, Z. Sun, A. Slesarev, L.B. Alemany, W. Lu and J.M. Tour, Improved synthesis of graphene oxide, *ACS Nano* **4**, 2010, 4806–4814.
- [4] C. Yu, C.-F. Wang and S. Chen, Facile access to graphene oxide from ferro-induced oxidation, *Sci. Rep-UK* **6**, 2016, 17071.
- [5] J. Chen, B. Yao, C. Li and G. Shi, An improved Hummers method for eco-friendly synthesis of graphene oxide, *Carbon* **64**, 2013, 225–229.
- [6] M.d.P. Lavin-Lopez, A. Romero, J. Garrido, L. Sanchez-Silva and J.L. Valverde, Influence of different improved Hummers method modifications on the characteristics of graphite oxide in order to make a more easily scalable method, *Ind. Eng. Chem. Res.* **55**, 2016, 12836–12847.
- [7] L. Peng, Z. Xu, Z. Liu, Y. Wei, H. Sun, Z. Li, X. Zhao and C. Gao, An iron-based green approach to 1-h production of single-layer graphene oxide, *Nat. Commun.* **6**, 2015, 5716.
- [8] J. Guerrero-Contreras and F. Caballero-Briones, Graphene oxide powders with different oxidation degree, prepared by synthesis variations of the Hummers method, *Mater. Chem. Phys.* **153**, 2015, 209–220.
- [9] C. Botas, P. Álvarez, P. Blanco, M. Granda, C. Blanco, R. Santamaría, L.J. Romasanta, R. Verdejo, M.A. López-Manchado and R. Menéndez, Graphene materials with different structures prepared from the same graphite by the Hummers and Brodie methods, *Carbon* **65**, 2013, 156–164.
- [10] W.S. Hummers, Jr. and R.E. Offeman, Preparation of graphitic oxide, *J. Am. Chem. Soc.* **80**, 1958, 1339, 1339.
- [11] M. Wojtoniszak and E. Mijowska, Controlled oxidation of graphite to graphene oxide with novel oxidants in a bulk scale, *J. Nanopart. Res.* **14**, 2012, 1248.
- [12] W.S. Hummers, Jr. and R.E. Offeman, Preparation of graphitic oxide, *J. Am. Chem. Soc.* **80**, 1958, 1339.
- [13] S. Park, J. An, J.R. Potts, A. Velamakanni, S. Murali and R.S. Ruoff, Hydrazine-reduction of graphite-and graphene oxide, *Carbon* **49**, 2011, 3019–3023.
- [14] L. Stobinski, B. Lesiak, A. Malolepszy, M. Mazurkiewicz, B. Mierzwa, J. Zemek, P. Jiricek and I. Bieloshapka, Graphene oxide and reduced graphene oxide studied by the XRD, TEM and electron spectroscopy methods, *J. Electron Spectrosc. Relat. Phenom.* **195**, 2014, 145–154.

- [15] B. Warren, X-ray diffraction in random layer lattices, *Phys. Rev.* **59**, 1941, 693.
- [16] T.A. Saleh, Applying Nanotechnology to the Desulfurization Process in Petroleum Engineering, 2015, IGI Global.
- [17] T.A. Saleh and V.K. Gupta, Nanomaterial and Polymer Membranes: Synthesis, Characterization, and Applications, 2016, Elsevier.
- [18] D.M. Crumpton, R.A. Laitinen, J. Smieja and D.A. Cleary, Thermal analysis of carbon allotropes: an experiment for advanced undergraduates, *J. Chem. Educ.* **73**, 1996, 590-591.
- [19] J. Chen, Y. Zhang, M. Zhang, B. Yao, Y. Li, L. Huang, C. Li and G. Shi, Water-enhanced oxidation of graphite to graphene oxide with controlled species of oxygenated groups, *Chem. Sci.* **7**, 2016, 1874-1881.
- [20] S. Eigler, C. Dotzer, F. Hof, W. Bauer and A. Hirsch, Sulfur species in graphene oxide, *Chem. A Eur. J.* **19**, 2013, 9490-9496.
- [21] T. Sun, S. Fabris and S. Baroni, Surface precursors and reaction mechanisms for the thermal reduction of graphene basal surfaces oxidized by atomic oxygen, *J. Phys. Chem. C* **115**, 2011, 4730-4737.
- [22] R. Rozada, J.I. Paredes, S. Villar-Rodil, A. Martínez-Alonso and J.M. Tascón, Towards full repair of defects in reduced graphene oxide films by two-step graphitization, *Nano Res.* **6**, 2013, 216-233.
- [23] J. Klimeš, D.R. Bowler and A. Michaelides, Chemical accuracy for the van der Waals density functional, *J. Phys. Condens. Matter* **22**, 2009, 022201.
- [24] C. Sun, Y. Feng, Y. Li, C. Qin, Q. Zhang and W. Feng, Solvothermally exfoliated fluorographene for high-performance lithium primary batteries, *Nanoscale* **6**, 2014, 2634-2641.
- [25] S. Drewniak, R. Muzyka, A. Stolarczyk, T. Pustelny, M. Kotyczka-Morańska and M. Setkiewicz, Studies of reduced graphene oxide and graphite oxide in the aspect of their possible application in gas sensors, *Sensors* **16**, 2016, 103.
- [26] T.A. Saleh, The influence of treatment temperature on the acidity of MWCNT oxidized by HNO₃ or a mixture of HNO₃/H₂SO₄, *Appl. Surf. Sci.* **257**, 2011, 7746-7751.
- [27] T.A. Saleh, A. Sari and M. Tuzen, Effective adsorption of antimony (III) from aqueous solutions by polyamide-graphene composite as a novel adsorbent, *Chem. Eng. J.* **307**, 2017, 230-238.
- [28] H. Wang and Y.H. Hu, Effect of oxygen content on structures of graphite oxides, *Industrial Eng. Chem. Res.* **50**, 2011, 6132-6137.
- [29] A. Alazmi, S. Rasul, S.P. Patole and P.M. Costa, Comparative study of synthesis and reduction methods for graphene oxide, *Polyhedron* **116**, 2016, 153-161.
- [30] J. Gao, F. Liu, Y. Liu, N. Ma, Z. Wang and X. Zhang, Environment-friendly method to produce graphene that employs vitamin C and amino acid, *Chem. Mater.* **22**, 2010, 2213-2218.
- [31] V. Loryuenyong, K. Totepvimarn, P. Eimburanaprat, W. Boonchompoo and A. Buasri, Preparation and characterization of reduced graphene oxide sheets via water-based exfoliation and reduction methods, *Adv. Mat. Sci. Eng.* **2013**, 2013, 5.
- [32] C.K. Chua and M. Pumera, The reduction of graphene oxide with hydrazine: elucidating its reductive capability based on a reaction-model approach, *Chem. Commun.* **52**, 2016, 72-75.
- [33] T. Soltani and B.-K. Lee, Low intensity-ultrasonic irradiation for highly efficient, eco-friendly and fast synthesis of graphene oxide, *Ultrason. Sonochem.* **38**, 2017, 693-703.
- [34] Y. Dong, J. Li, L. Shi, J. Xu, X. Wang, Z. Guo and W. Liu, Graphene oxide-iron complex: synthesis, characterization and visible-light-driven photocatalysis, *J. Mater. Chem. A* **1**, 2013, 644-650.
- [35] T.A. Saleh, M.M. Al-Shalalfeh and A.A. Al-Saadi, Graphene Dendrimer-stabilized silver nanoparticles for detection of methimazole using Surface-enhanced Raman scattering with computational assignment, *Sci. Rep. UK* **6**, 2016, 32185.
- [36] R.S. Edwards and K.S. Coleman, Graphene synthesis: relationship to applications, *Nanoscale* **5**, 2013, 38-51.
- [37] H. Gao, K. Zhu, G. Hu and C. Xue, Large-scale graphene production by ultrasound-assisted exfoliation of natural graphite in supercritical CO₂/H₂O medium, *Chem. Eng. J.* **308**, 2017, 872-879.
- [38] G. Wang, X. Shen, B. Wang, J. Yao and J. Park, Synthesis and characterisation of hydrophilic and organophilic graphene nanosheets, *Carbon* **47**, 2009, 1359-1364.
- [39] Y. Zhu, S. Murali, W. Cai, X. Li, J.W. Suk, J.R. Potts and R.S. Ruoff, Graphene and graphene oxide: synthesis, properties, and applications, *Adv. Mater.* **22**, 2010, 3906-3924.
- [40] M.M. Lucchese, F. Stavale, E.H.M. Ferreira, C. Vilani, M.V.O. Moutinho, R.B. Capaz, C.A. Achete and A. Jorio, Quantifying ion-induced defects and Raman relaxation length in graphene, *Carbon* **48**, 2010, 1592-1597.

- [41] I. Suresh, K. Chidambaram, V. Vinod, N. Rajender, R.M. Venkateswara and Č. Miroslav, Synthesis, characterization and optical properties of graphene oxide-polystyrene nanocomposites, *Polym. Adv. Technol.* **26**, 2015, 214-222.
- [42] J. He and L. Fang, Controllable synthesis of reduced graphene oxide, *Curr. Appl. Phys.* **16**, 2016, 1152-1158.
- [43] T. Szabó, A. Szeri and I. Dékány, Composite graphitic nanolayers prepared by self-assembly between finely dispersed graphite oxide and a cationic polymer, *Carbon* **43**, 2005, 87-94.
- [44] H.J. Shin, K.K. Kim, A. Benayad, S.M. Yoon, H.K. Park, I.S. Jung, M.H. Jin, H.K. Jeong, J.M. Kim and J.Y. Choi, Efficient reduction of graphite oxide by sodium borohydride and its effect on electrical conductance, *Adv. Func. Mater.* **19**, 2009, 1987-1992.
- [45] N. Morimoto, T. Kubo and Y. Nishina, Tailoring the oxygen content of graphite and reduced graphene oxide for specific applications, *Sci. Rep-UK* **6**, 2016, 21715.
- [46] T.-Y. Zhang and D. Zhang, Aqueous colloids of graphene oxide nanosheets by exfoliation of graphite oxide without ultrasonication, *Bull. Mater. Sci.* **34**, 2011, 25-28.
- [47] Y. Hernandez, V. Nicolosi, M. Lotya, F.M. Blighe, Z. Sun, S. De, I. McGovern, B. Holland, M. Byrne and Y.K. Gun'Ko, High-yield production of graphene by liquid-phase exfoliation of graphite, *Nat. Nanotechnol.* **3**, 2008, 563-568.

Graphical abstract

Graphical Abstrac:



alt-text: Image

Highlights

- A environmentally friendly oxidant to synthesized Graphite Oxide is proposed.
- Result was compared with Graphite Oxide synthesized by the Improved Hummer Method.
- A less oxidized GrO, which could be useful for several applications, was obtained.
- Graphene Oxide (GO) and Reduced Graphene Oxide (RGO) were obtained from both GrO.

Queries and Answers

Query: Please confirm that given names and surnames have been identified correctly and are presented in the desired order and please carefully verify the spelling of all authors' names.

Answer: Yes

Query: Your article is registered as a regular item and is being processed for inclusion in a regular issue of the journal. If this is NOT correct and your article belongs to a Special Issue/Collection please

contact p.kumar.7@elsevier.com immediately prior to returning your corrections.

Answer: Yes